Laboratory Studies of the Chemistry of Transneptunian Object Surface Materials

R. L. Hudson
Eckerd College and NASA Goddard Space Flight Center

M. E. Palumbo and G. Strazzulla
INAF-Osservatorio Astrofisico di Catania

M. H. Moore, J. F. Cooper, and S. J. Sturner
NASA Goddard Space Flight Center

Bombardment by cosmic-ray and solar wind ions alters the surfaces of transneptunian objects (TNOs) surfaces, and the influence of this weathering on candidate TNO materials has been extensively examined by laboratory scientists. Low-temperature radiation experiments with icy materials have demonstrated the existence of a rich TNO ice chemistry involving molecules such as H_2O, CH_4, N_2, and NH_3. These same experiments have provided insight into reaction mechanisms needed to predict yet-unseen chemical species. Near-IR and visible spectra of ion-irradiated candidate refractories have generated the data needed to understand TNO colors and spectral slopes. The planning, execution, and interpretation of these experiments have been influenced by new energetic particle measurements from Voyager and other heliospheric spacecraft and by models for TNO surface irradiation fluxes and dosages. Experiments and available surface irradiation models suggest specific timescales for reddening of TNO surfaces. Altogether, laboratory investigations and heliospheric radiation measurements contribute to the study of TNOs by aiding in the interpretation of astronomical observations, by suggesting new lines of investigation, and by providing the underlying knowledge needed to unravel the chemical and spectral evolution of objects in the outer solar system.

1. INTRODUCTION

The objects in the outer solar system can be organized into three different groups according to their observed surface IR spectra. First are objects with spectra dominated by H_2O-ice, such as some Centaurs, Charon, and several transneptunian objects (TNOs). A second group has spectra with prominent CH_4 features, and includes Triton, Pluto (both also have N_2-ice), and several TNOs. A third group includes objects having featureless spectra. This spectral diversity clearly indicates compositional differences in surface layers to a few millimeters or less in depth. More speculative are the compositions of the underlying layers and the processes by which they contribute material to TNO surfaces. For example, water ice may come from Enceladus-like outgassing (*Porco et al.,* 2006; *Waite et al.,* 2006), CH_4 could either be of internal primordial origin or be produced by surface irradiation, and more neutral featureless spectra could arise from long cumulative irradiation (*Moroz et al.,* 2003, 2004).

At present, six molecules (H_2O, CH_4, N_2, NH_3, CO, and CH_3OH) suffice to explain the spectral bands of icy TNO terrains. In addition, silicates and complex organics, presumably highly processed by cosmic radiation and/or micrometeorite bombardment, can explain spectral slopes and colors in the UV, visible, and near-IR regions. However, it is a challenge to reconcile these surface compositions with bulk compositions, as inferred from gas-phase observations of comets near the Sun. Note that the comets of the Jupiter family (i.e., coming from the Oort cloud) have compositions similar to those believed to have originated in the Kuiper belt. Within the current inventory of about 50 cometary molecules, nuclear ices are dominated by H_2O, CO, CO_2, and minor species such as CH_3OH, H_2CO, and CH_4. Some compositional differences among TNOs, comets, and other icy objects at the edge of the solar system can be understood in part by variations in formation and storage temperatures, which affect vapor pressure, and mass, which affects escape velocity. However, a complex evolutionary history for outer solar system objects is thought to include stochastic events as well as continuous exposure to ionizing radiation. The subject of this chapter is the use of laboratory data, theory, and spacecraft measurements to understand how long-term radiation exposure causes chemical changes in TNO ices and non-icy TNO surface materials.

Three observations are consistent with energetic processing of outer solar system objects. First, the visible and near-IR spectra of TNOs and ion-irradiated laboratory materials have similar slopes, which differ from those of ices and refractories that have not been irradiated (*Brunetto et al.,* 2006). Another observation is the detection of abundant C_2H_6 in comets C/1996 B2 Hyakutake (*Mumma et al.,* 1996) and C/1995 O1 Hale-Bopp (*Weaver et al.,* 1998). A C_2H_6 abundance comparable with that of CH_4 implies that these

comets' ices did not originate in a thermochemically equilibrated region of the solar nebula, but were produced by processing of icy interstellar grain mantles. Both comets are thought to be Oort cloud objects with an origin somewhere in the Jupiter–Neptune region. Finally, the low surface reflectance and the neutral featureless color spectra of many objects are as expected from millions to billions of years of cosmic ray irradiation, if the most highly irradiated outer surface is not removed by plasma sputtering or meteoritic impacts (*Cooper et al.,* 2003, 2006a; *Strazzulla et al.,* 2003).

Over the past 30 years, laboratory research has shown that high-energy particles and photons cause irreversible physical and chemical changes in relevant solar system ices and analog surface materials. Since solar system surfaces have been exposed to radiation and have been altered over time, laboratory experiments can be used to investigate and predict radiation chemical changes.

In this chapter we summarize the results of many radiation chemistry experiments on relevant TNO ices and other surface materials. Based on past successes, a comprehensive picture of radiation processing is emerging, one that can be used to predict radiation products to be sought in upcoming missions and observing campaigns.

2. LABORATORY APPROACH

Assignments of TNO spectral features are based on comparisons to the spectra of materials available in laboratories (see chapter by de Bergh et al.). However, the alteration of TNO surfaces by energetic photons and ions means that specific experiments are needed to probe the resulting chemical and physical changes.

At present there are several laboratories where research is conducted to study processes, such as ion irradiation and UV photolysis, which can drive the evolution of TNO surface materials, such as ices, silicates, and carbonaceous solids. In the case of ices, experiments usually begin with the preparation of a sample by condensation of an appropriate gas, or gas-phase mixture, onto a 10–300 K substrate in a high or ultrahigh vacuum chamber (P ~ 10^{-7}–10^{-11} mbar). The ice's thickness can be measured by monitoring the interference pattern (intensity vs. time) from a laser beam reflected both by the vacuum-film and film-substrate interfaces (e.g., *Baratta and Palumbo,* 1998). The icy film produced can be processed by keV and MeV ions and electrons or by far-UV photons (e.g., Lyman-α, 10.2 eV). The resulting chemical and physical changes can be followed with visible, IR, and Raman spectroscopies before, during, and after processing. Experimental setups used to study refractory materials, such as silicates and carbonaceous compounds, are similar to those used to investigate ices.

Several different types of processing experiments have been performed. If the sample is thinner than the penetration depth of the impinging ions or photons, then they pass through the target. In some such cases the resulting spectrum shows only the more-intense IR absorptions. To enhance the weaker bands, irradiation can be done during sample deposition, building up a larger thickness of processed material. Finally, if the sample thickness is greater than the penetration depth of incident ions or photons, only the uppermost layers of the sample are altered. If the projectile is a reactive species, such as an H, C, N, O, or S ion, then it can be implanted into the ice to form new molecules that include the projectile.

Ions impinging on solids release energy mainly through elastic collisions with target nuclei, and inelastic interactions that cause the excitation and ionization of target species. For keV and MeV ion irradiations, doses can be estimated from a knowledge of the ion fluence (ions cm^{-2}), the energy of impinging ions (eV), the stopping power (eV/Å or eV cm^2 $molecule^{-1}$), and the penetration depth or range of the chosen projectiles (Å or molecules cm^{-2}). The ion energy and fluence are measured during laboratory irradiation, while the stopping power and range can be calculated, for example, with Ziegler's SRIM program (*www.srim.org*) (*Ziegler et al.,* 1985). In these experiments, low current densities, such as 0.001–1 μA cm^{-2}, are used to avoid macroscopic heating of the target. To facilitate comparisons between different samples and different energy sources, most workers use eV/16-amu-molecule as a standard unit of dose, even in UV-photolysis experiments. This unit is sometimes abbreviated, with occasional ambiguity, as eV/molecule. Note that 100 eV/16-amu at unit density corresponds to 60 gigarads, a dose that produces significant change in the bulk chemistry of irradiated materials.

Although laboratory experiments are commonly done with keV and MeV radiations, for theoretical models it is sometimes necessary to consider interactions at higher energies. For the MeV-to-GeV range, the GEANT radiation transport code, which includes secondary and higher-order interactions, is available at *wwwasd.web.cern.ch/wwwasd/geant* (*Sturner et al.,* 2003).

Irradiated samples can be analyzed by (1) near- and mid-IR transmission spectroscopy, in which case an IR-transparent substrate is used, such as KBr, CsI, or crystalline silicon; (2) transmission-reflection-transmission IR spectroscopy, in which case a substrate that reflects the IR beam, such as Al or Au, is used; (3) visible and near-IR diffuse reflectance spectroscopy, in which case an optically rough, diffusing Au substrate is used; and (4) Raman spectroscopy. Although laboratory Raman spectra cannot be directly compared with astronomical visible and IR observations, they provide valuable information on solid-phase radiation effects, in particular structural changes in carbonaceous materials and carbon-rich ice mixtures. Furthermore, because of the different selection rules that govern the interaction of light and matter in the IR and Raman techniques, these spectra give complementary information.

Additional details concerning experimental procedures can be found in *Baratta and Palumbo* (1998), *Palumbo et al.* (2004), *Moore and Hudson* (2003), *Gerakines et al.* (2005), and *Bernstein et al.* (2005).

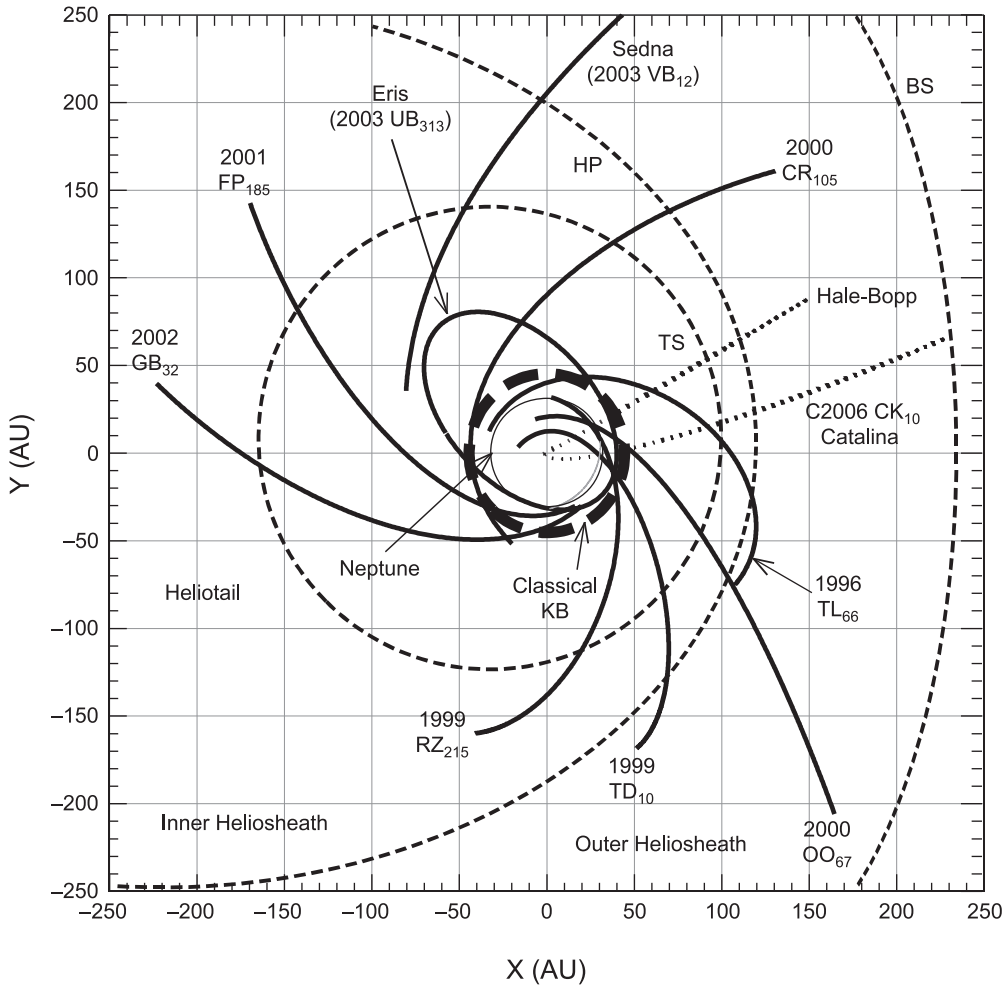

Fig. 1. Trajectories (solid curves) of selected TNOs and inner Oort cloud comets with highly eccentric orbits, many crossing the solar wind termination shock (TS). Other heliospheric boundaries (dashed curves) and regions include the inner heliosheath, heliopause (HP), outer heliosheath, and the bow shock (BS). See *Cooper et al.* (2006a) for more details on coordinates and boundaries.

3. RADIATION ENVIRONMENT

Since TNO surfaces are altered by exposure to high-energy particles and photons, it is important to understand the fluxes, energies, and distribution of radiations in the outer solar system. These have been studied with a combination of theoretical modeling and *in situ* measurements by spacecraft. Figure 1 shows the relevant parts of the heliosphere (region of the Sun's influence on plasma environment) and the solar system, with orbits of selected TNOs and other objects superimposed. Pioneers 10 and 11 combined to probe the 30–80-AU region, but ceased data return in 1995 and 2002, respectively. The solar wind plasma and energetic particle radiation environments beyond Neptune's 30-AU orbit were directly measured by Voyager 1 (only energetic particles due to failure of the plasma instrument in 1980), in 1987, and Voyager 2, in 1989 (*Cooper et al.,* 2003). Knowledge of the outer heliospheric environment dramatically advanced when Voyager 1 crossed the solar wind termination shock at 94 AU in December 2004 (*Burlaga et al.,* 2005; *Decker et al.,* 2005; *Stone et al.,* 2005). This boundary, labeled TS in Fig. 1, marks the transition from supersonic to subsonic flow of solar wind plasma.

Beyond the termination shock in the outer solar system is the heliopause, the theoretical boundary near minimum distance 120 AU between outward-flowing solar wind plasma and inflowing plasma of the local interstellar medium (LISM). Voyager 1 is currently passing through the intervening inner heliosheath region, while Voyager 2 is expected to enter it within the current decade. Some theoretical models suggest that interstellar plasma flowing inward across a theoretical bow shock (BS in Fig. 1) into the outer heliosheath region may also undergo a sonic transition.

The classical Kuiper belt, beyond the orbit of Neptune as shown in Fig. 1, now resides far sunward of the termination shock, although the latter may have occasionally have moved further inward in response to changes in the local interstellar environment of the Sun. More than 30

scattered disk objects have highly eccentric orbits traversing the termination shock in various directions (*Cooper et al.,* 2006a), and a few of these objects, in addition to more than 300 known comets, travel as far as the heliopause and the interstellar plasma environment beyond.

On going away from the Sun, the proton energy flux decreases and reaches a broad minimum in the middle of the supersonic heliosphere (upwind of TS), including the classical Kuiper belt region at 30–50 AU. This holds true over a large range of energy values. At even greater distances from the Sun, there is an increase in flux in going from the middle heliosphere to the inner heliosheath and then beyond into the local interstellar medium. *Cooper et al.* (2006a) have suggested that since the measured inner heliosheath spectrum is approaching that of a LISM model spectrum then the actual source may be in the interstellar environment beyond an ion-permeable heliopause. If so, a complete quantitative model for irradiation of TNOs in near-circular and highly eccentric orbits, as illustrated in Fig. 1, may be within reach.

As already stated, a common feature among TNOs is their exposure to energetic ions (mostly H^+, He^+, and O^+) and solar UV photons that slowly modify the chemistry of surface materials. Compositional abundances of solar wind plasma and energetic ions in the heliosphere are mostly similar to those of the solar photosphere (*Anders and Grevesse,* 1989), but there can be additional sources from solar, heliospheric, and galactic acceleration processes. Low-energy protons and heavier ions contribute to alteration of surface chemistry by direct implantation, while more energetic (keV–MeV) ions become important for inducing radiation-chemical reactions (see the following section) and sputtering of outer molecular layers (*Johnson,* 1990, 1995). Radiolytic chemical alteration of TNO surface ices at millimeter-to-meter depths is primarily driven by high-energy (keV–GeV) protons as the result of primary and secondary interactions (*Cooper et al.,* 2003, 2006a). Electrons are more penetrating than protons or ions of the same energy and may have significant radiolytic effects even at plasma energies. Figure 2 shows stopping range and differential energy loss rates for protons, selected heavier ions, and electrons as extended to lower energies from data above 10 keV (*Cooper et al.,* 2001) (note that the axis units in Figs. 12 and 13 of the latter reference were incorrectly labeled).

Vacuum-UV solar photons have a complex spectrum at 1 AU (*Hall et al.,* 1985; *Tobiska,* 2000; *Tobiska and Bouwer,* 2006). Their energy flux is generally higher than that from charged particles, except within the intense trapped radiation belt environment of the jovian magnetosphere (*Cooper et al.,* 2001). However, the UV penetration depth is only ~0.15 μm, as compared to the ~100-μm thickness of ice sampled by near-IR observations, so UV photolysis products can be removed by surface erosion or highly altered by radiation processing. Alternatively, UV photons can initiate gas-phase photochemistry on Pluto-sized TNOs with atmospheres (*Elliot and Kern,* 2003), and the reaction products can precipitate downward to potentially dominate surface compositions.

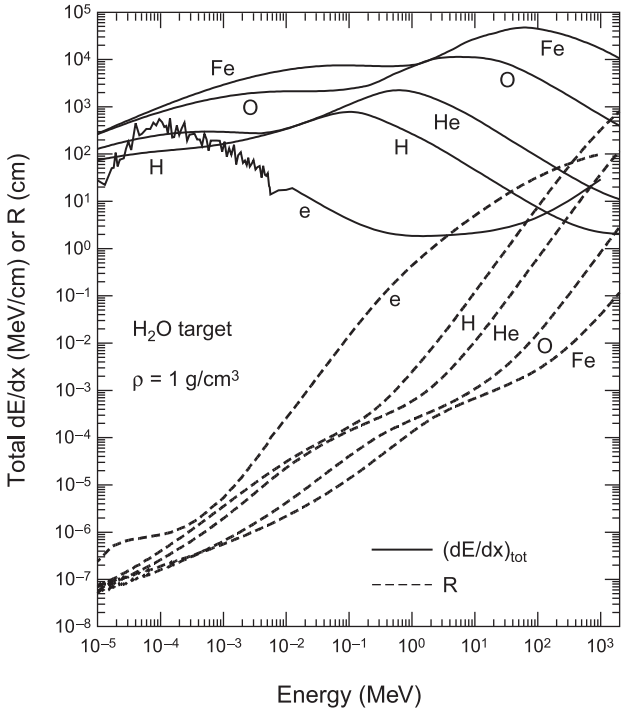

Fig. 2. Stopping ranges (R) and differential energy loss rates (dE/dx) in water at unit density of protons (H), the indicated heavier ions (He-Fe), and electrons (e). The loss rate is the sum of atomic ionization and nuclear collision components for protons and ions. For electrons, dE/dx is the sum of ionization and radiative energy losses. Proton and ion data are from the SRIM model (*Ziegler et al.,* 1985; *www.srim.org*). Electron data above 1 keV are from the ESTAR database (*physics.nist.gov/PhysRefData/Star/Text/ESTAR.html*) and at lower energies from published data for polystyrene at nearly (1.05 g/cm^3) unit density (*X-Ray Data Booklet,* Lawrence Berkeley National Laboratory, 2001).

Table 1 gives estimates of the doses accumulated in 4.6 G.y. by the outer 1 μm, 100 μm, and 1 m of an ice with an assumed density of 1 g cm^{-3} (*Cooper et al.,* 2003,2006a). Objects in a broad zone of the middle heliosphere, around 40 AU, experience moderate irradiation from galactic cosmic-ray ions at micrometer-to-meter depths (Pluto and dynamically cold TNOs). This region is bounded on the sunward side by increasing fluxes of solar energetic ions, resulting in increased surface doses for Centaurs. On the antisunward side there are rising fluxes of energetic ions diffusing inward from the heliosheath and perhaps also from the LISM. *Cooper et al.* (2003) have suggested that this radial separation of internal and outer heliospheric ion sources provides a potential explanation for predominately red colors of the more ancient objects in low-inclination, low-eccentricity orbits beyond 40 AU. That is, these red objects are less irradiated than those in other regions either closer to or further away from the Sun.

TABLE 1. Estimated radiation doses (eV/16-amu molecule) for ice-processing environments*,†.

Object	Ices Detected	Distance (AU)	Dose at 1-μm Depth†	Dose at 100-μm Depth†	Dose at 1-m Depth†
Centaur	H_2O, CH-containing ices (CH_3OH?), silicates, organics ("tholin")	5–35	100‡–10,000§	100‡–200§	30‡
		48–1000	100‡–500,000¶	100‡–30,000¶	30‡–50¶
Triton	N_2, CH_4, CO, CO_2, H_2O				
Pluto	N_2, CH_4, CO (and H_2O?)	30–40	100‡	100‡	30‡
Charon	H_2O, NH_3, NH_3-hydrate				
TNO	H_2O, CH_4, NH_3, NH_3-hydrate?	<48	100‡	100‡	30‡
		~1000	500,000¶	30,000¶	50¶
Oort cloud comet	Gases**: H_2O, CO, CO_2, CH_3OH, CH_4, H_2CO, NH_3, OCS, HCOOH, HCN, C_2H_6, C_2H_2	~40,000–100,000	500,000¶	30,000¶	50¶

*Doses in eV (16-amu molecule)$^{-1}$ for 4.6 G.y., with an ice density of 1.0 g cm^{-3}.
†Solar minimum.
‡*Cooper et al.* (2003) extended with GEANT.
§J. F. Cooper et al. (unpublished data, 2006).
¶*Cooper et al.* (2006a).
**The assumed origin of these gases is the comet's nucleus.

It is important to note that the doses in Table 1 are based on direct observations of ion fluxes and on well-established theories of ion-matter interactions. Thus the processes that are studied in the laboratory must necessarily apply to the objects of Table 1, and will compete with resurfacing, collisional evolution, and micrometeoritic bombardment.

4. SPECTROSCOPY AND TRANSNEPTUNIAN OBJECT CHEMISTRY

Studies of TNO chemistry have been dominated by two interconnected approaches, astronomical observations and laboratory experiments. While polarization and photometry measurements have been valuable for understanding TNO density and porosity (e.g., *Bagnulo et al.,* 2006), spectroscopy has been the method of choice for probing TNO chemistry. Most TNO spectra have been measured at visible and near-IR wavelengths where the cold surfaces efficiently reflect solar radiation. [For an exception, see *Grundy et al.* (2002) for mid-IR data.] Visible-light measurements alone, and even some combined with near-IR data, usually give only sloping featureless spectra making unique chemical assignments difficult. These spectra will be examined more thoroughly in section 5.

The only firm assignments of TNO spectral features to specific molecules have come from near-IR data (see the chapter by Barucci et al.). As an example, the reflectance spectrum of Quaoar (*Jewitt and Luu,* 2004) exhibits absorptions near 1.5 and 2.0 μm that are characteristic of H_2O-ice, and a small dip at 1.65 μm shows that the ice is crystalline and at a temperature below 80 K. Evidence of an ammonia (NH_3) species comes from a small feature near 2.2 μm. The near-IR spectrum of Charon exhibits the same H_2O-ice bands (*Brown and Calvin,* 2000). Contrasting with these objects are Pluto and 2005 FY_9, whose near-IR spectra indicate the presence of CH_4-ice (*Licandro et al.,* 2006).

Other species considered in the analysis of TNO near-IR spectra include cyanides, both organic and inorganic (*Trujillo et al.,* 2007), and hydrocarbons (*Sasaki et al.,* 2005), although no firm spectral assignments to specific molecules have yet been published. The Centaur 5145 Pholus is thought to have originated in the Kuiper belt, and models show that solid CH_3OH (methanol) may be among its surface ices (*Cruikshank et al.,* 1998). A long series of near-IR observations of Pluto and Triton have revealed that they possess multicomponent ice surfaces. In addition to CH_4, both solid N_2 and CO have been detected on Pluto, with N_2 dominating in some regions and CH_4 in others (*Douté et al.,* 1999). For Triton, N_2, CH_4, and CO are also observed, but H_2O- and CO_2-ice features are suggested by the data as well (*Quirico et al.,* 1999).

All these TNO observations have motivated laboratory work whose goal is to record near-IR spectra of single- and multicomponent ices at temperatures relevant to the outer solar system. The work of Schmitt and colleagues has produced a collection of spectra and optical constants of single-component ices, and these data are treated elsewhere (see the chapter by de Bergh et al.). Near-IR band strengths have been published recently by *Gerakines et al.* (2005) for many TNO-relevant molecules. New spectra and band strengths of ice mixtures made from H_2O, CO_2, CH_4, and CH_3OH are also available (*Bernstein et al.,* 2005, 2006).

Here we consider the likely solid-phase chemistry of some known and suspected TNO molecules, with spectros-

copy as the major investigative tool. The three types of ices to be considered are those made of a single component, those made of mixtures dominated by a very polar molecule (H_2O), and those made of mixtures dominated by a nonpolar material (N_2). The primary goal motivating the laboratory work is the discovery of efficient reactions leading from simple starting materials to more-complex species, to allow predictions of as-yet-unobserved TNO molecules.

4.1. Radiation Chemistry and Transneptunian Object Ices

Chemical reactions in TNO ices can be initiated both by solar far-UV photons, with energies in the 5–120-eV (250–5-nm) range, and cosmic-ray ion bombardment, with energies in the keV–MeV region and higher. Despite this great variation in energy, similar chemical products result from the two processes. The reason for this is that MeV radiation interacts with matter through a series of discrete steps, each involving energy loss until the eV level is reached (*Johnson,* 1990). Specifically, a single 1-MeV H^+ cosmic ray passing through an ice loses energy through the production of secondary electrons, which in turn lead to thousands of ionizations and excitations in the ice. These events result in the breakage of chemical bonds and the rearrangement of molecular fragments to give new molecules and ions. These eV-level ionizations and excitations resemble those of conventional UV photochemistry, so that the final products of photo- and radiation chemistry are quite similar, when comparable energy doses are involved. Differences do exist, however, as keV–MeV radiation is far more penetrating than UV photons, and can produce opaque surface materials that prevent penetration by UV or visible light (*Baratta et al.,* 2002). Note also that the chemical products from various MeV radiations (e.g., H^+, He^+, e^-, X-rays, γ-rays) acting on ices are essentially indistinguishable since it is the secondary electrons that cause the bulk of the chemical change, masking the identity of the original radiation. Finally, there are a few molecules, such as N_2, that are not dissociated by far-UV photons in a single step. In such cases the molecule can still be excited and react with other species, or vice versa, which may or may not result in dissociation. See *Moore and Hudson* (2003) for an example, the formation of DCN from both the ion irradiation and the UV photolysis of $N_2 + CD_4$ ices.

Table 1 of the previous section lists radiation doses thought to be typical for TNOs. Over several billion years every molecule within about 100 μm of a TNO's surface will receive 10^1–10^5 eV, depending on solar system position and heliospheric activity. A relatively constant 30–50 eV/molecule occurs everywhere at meter depths, due to very-high-energy galactic cosmic rays that are little affected by solar modulation. These doses are attainable in laboratories, and so experiments can be performed to explore radiation chemical reactions of TNO analog materials. We now survey some of the published literature on the low-temperature chemistry of TNO molecules.

4.2. Chemistry of Single-Component Ices

Spectroscopic detections of extraterrestrial H_2O-ice have been based on far-, mid-, and near-IR spectra. Features in the far-IR region arise from intermolecular transitions and are quite sensitive to the amorphous or crystalline nature of the ice. Mid-IR features of H_2O, and all other molecules, arise from characteristic intramolecular fundamental vibrations of groups of atoms. Near-IR bands, which have permitted identifications of specific ice molecules on TNO surfaces, arise from overtones and combinations of a molecule's fundamental vibrations. Near-IR bands are typically an order of magnitude weaker than those in the mid-IR.

Of these three spectral regions, laboratory workers studying reaction chemistry typically use the mid-IR as it is the most reliable for identification of product molecules. In contrast, TNO observers favor near-IR spectra. Here we consider both regions, but with an emphasis on results from the mid-IR to suggest with confidence the reaction products that one might expect in TNO ices.

The first ice reported on a classical TNO was H_2O (*Brown et al.,* 1999). Knowing that this ice is present, and that TNOs exist in a radiation environment, what other molecules might one reasonably expect to be present? Irradiated H_2O-ice has been studied for about a century, and still attracts attention. Early experiments showed that the molecular products of H_2O-ice decomposition, both by photo- and radiation chemistry, are H_2, O_2, and H_2O_2, as expected. In both photolysis and radiolysis, H_2 and H_2O_2 are thought to form by combination of radical-radical reactions, as indicated below.

$$H_2O \rightarrow H + OH \text{ (twice)}$$
$$OH + OH \rightarrow H_2O_2$$
$$H + H \rightarrow H_2$$

The mechanism for O_2 formation is still being studied, and recent work strongly suggests that trapped oxygen atoms are necessary precursors to O_2 formation (*Johnson et al.,* 2005).

Since H_2 and O_2 lack permanent dipole moments, their fundamental vibrational transitions are very weak, and do not lead to pronounced spectral features, leaving H_2O_2 as the most easily detectable product. Near-IR spectra of frozen H_2O_2 and H_2O_2-H_2O mixtures have been recorded down to ~9 K, and the H_2O_2 bands are found to strongly overlap those of H_2O-ice (*Hudson and Moore,* 2006). This suggests that while H_2O_2 is a well-known product of H_2O-ice irradiation (e.g., *Loeffler et al.,* 2006a; *Gomis et al.,* 2004a,b; *Moore and Hudson,* 2000), its near-IR detection on a TNO will be difficult. A more-promising approach might be to seek the mid-IR band near 3.5 μm that was used to identify H_2O_2 on Europa (*Carlson et al.,* 1999a).

There are cases for which characteristic IR features of CH_4-ice can be observed on TNO surfaces (*Grundy et al.,* 2002). This leads to questions about the products that might arise from the low-temperature irradiation of methane. Relevant experiments have been performed by several research groups (e.g., *Mulas et al.,* 1998; *Moore and Hudson,* 2003;

Baratta et al., 2003), and the consensus appears to be that radical-radical reactions can lead to more-complex hydrocarbons. For C_2H_6 (ethane) formation, the key path appears to be

$$CH_4 \rightarrow CH_3 + H \text{ (twice)}$$
$$CH_3 + CH_3 \rightarrow C_2H_6$$

although insertion reactions such as

$$CH_4 \rightarrow CH_2 + H_2 \text{ (or 2 H)}$$
$$CH_2 + CH_4 \rightarrow C_2H_6$$

probably play a role as well. In addition to C_2H_6, experiments have shown that the radiation products of frozen CH_4 include small hydrocarbons such as C_2H_4, C_2H_2, and C_3H_8 (e.g., *Mulas et al.,* 1998; *Moore and Hudson,* 2003; *Baratta et al.,* 2003). Overall, the safest prediction is that C_2H_6, a dominant product, will be present in CH_4-rich TNO ices.

The third molecule that has been reported to dominate a TNO surface is molecular nitrogen. Like H_2 and O_2, it has no permanent dipole moment, so its vibrational transitions are weak. Nevertheless, direct detection of N_2-ice has been made on Pluto (*Owen et al.,* 1993) and Triton (*Cruikshank et al.,* 1993) through the first overtone band of N_2. The radiation chemistry of N_2 ices is far more limited than that of either H_2O or CH_4, and only N_3 has been identified as a radiation product (*Hudson and Moore,* 2002). This radical was detected after ion bombardment of N_2-ice, and was identified through a single mid-IR feature, which rapidly decayed above 35 K.

To illustrate radiation-induced changes in an organic compound, we consider methanol (CH_3OH). *Brunetto et al.* (2005) presented both reflectance and transmission near-IR spectra (2.2–2.4 μm) of CH_3OH-ice at 16 K and 77 K, before and after irradiation with 30 keV He^+ ions and 200 keV H^+ ions. Their results confirmed the CO and CH_4 formation known from mid-IR studies. They also found evidence for a strong decrease in the intensity of the CH_3OH band at ~2.34 μm relative to the one at 2.27 μm. Figure 3 illustrates these near-IR results for H^+ irradiation at 16 K. In addition to the appearance of new spectral features, there is a change in the underlying spectral slope, indicating an alteration of the sample's color. We return to this observation in section 5, and to the radiation products of CH_3OH in section 4.3.

Table 2 summarizes radiation products for a wide variety of pure molecules, drawn from independent work in several laboratories. Temperatures for many of the experiments were well below those of TNOs, but in most cases this will make no difference in the radiation chemistry, which is not thermally driven.

4.3. Chemistry of H_2O-rich Ice Mixtures

Radiation chemistry experiments have been reported for essentially all common classes of organic molecules embedded in a H_2O-rich ice. Table 3 updates an earlier list (*Colangeli et al.,* 2005), starting with H_2O-hydrocarbon

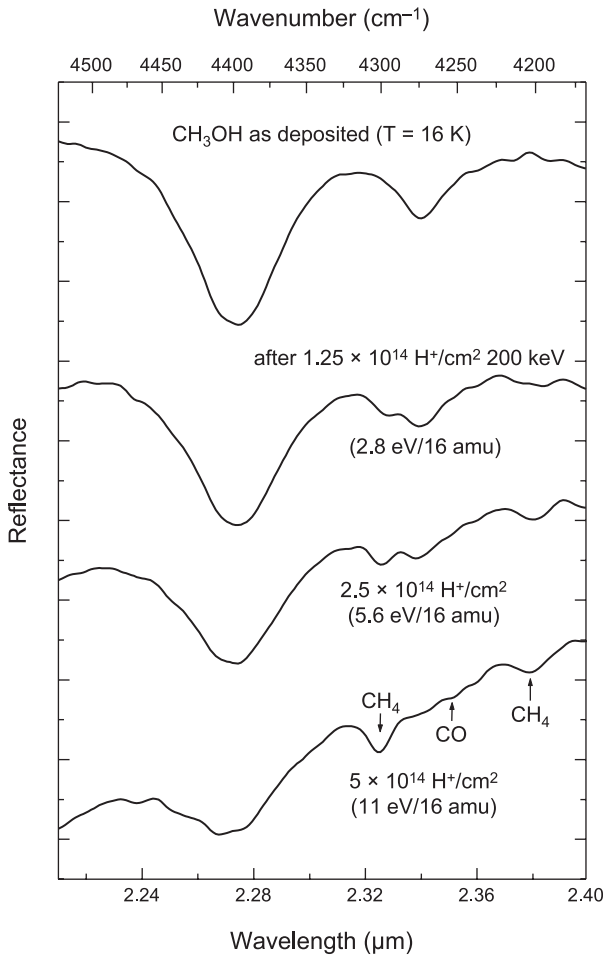

Fig. 3. Near-IR spectra of frozen CH_3OH before (top) and after various stages of irradiation, showing product formation. The four traces are offset for clarity (from *Brunetto et al.,* 2005).

mixtures. As with pure CH_4-ices, C_2H_6 is a radiation product in $H_2O + CH_4$ mixtures, which shows that H_2O does not block the reactions already given for methane. An important new product in these experiments is CH_3OH, thought to be made by radical-radical reactions as

$$CH_4 \rightarrow CH_3 + H$$
$$H_2O \rightarrow H + OH$$
$$CH_3 + OH \rightarrow CH_3OH$$

Recent work has shown that CH_2 insertion reactions such as

$$CH_4 \rightarrow CH_2 + H_2 \text{ (or 2 H)}$$
$$CH_2 + H_2O \rightarrow CH_3OH$$

also play a role in the CH_3OH formation (*Wada et al.,*2006). Spectra and selected band strengths for pure CH_3OH and $H_2O + CH_3OH$ mixtures are available to assist with analyzing TNO spectra (*Kerkhof et al.,* 1999), although optical constants are hard to locate (but see *Cruikshank et al.,* 1998).

Table 3 summarizes results for H_2O-rich mixtures containing the aforementioned radiation products, C_2H_6 and CH_3OH, of $H_2O + CH_4$ ices. If C_2H_6 is embedded in an

TABLE 2. Radiation products from one-component ices.

Ice	Reaction Products Identified in Ices	Least-Volatile Species	References
H_2O	H_2O_2	H_2O_2	[1,2,3,4]
CH_4	C_2H_2, C_2H_4, C_2H_6, C_3H_8, CH_3, C_2H_5	PAHs [4] and high molecular weight hydrocarbons	[5,6,7]
C_2H_6	CH_4, C_2H_2, C_2H_4	high molecular weight hydrocarbons	[8]
C_2H_4	CH_4 , C_2H_2, C_2H_6	high molecular weight hydrocarbons	[8]
C_2H_2	CH_4 [5], polyacetylene [8]	PAHs [4], polyacetylene [8]	[5,8,9]
CO	CO_2, C_3O_2, C_2O, C_4O, C_5O_2, C_7O_2	C_3O_2, C_5O_2, C_7O_2	[10,11,12]
CO_2	CO, O_3, CO_3	H_2CO_3 (from H^+ implantation) [11]	[10,13]
H_2CO	CO, CO_2, HCO, POM	polyoxymethylene (POM)	[14]
CH_3OH	CH_4, CO, CO_2, H_2CO, H_2O, $C_2H_4(OH)_2$, HCO, $HCOO^-$	$C_2H_4(OH)_2$	[15,16]
O_2	O_3		[9]
N_2	N_3		[17]
NH_3	NH_4^+	NH_4^+	[9,18]
HCN	HCN oligomers	HCN oligomers	[19]
CH_3CN	CH_4, H_2CCNH, CH_3NC, HCN	polymeric material	[20]
HCCCN	HCCNC (?)	polymeric material	[20]
HNCO	NH_4^+, OCN^-, CO, CO_2	NH_4OCN	[9]
SO_2	SO_3	S_8	[21,22]
H_2S	H_2S_2	H_2S_2	[22]
OCS	CO, CS_2	CS_2	[9]
$HC(O)CH_2OH$	CO, CO_2, CH_4, HCO, H_2CO, CH_3OH, $(CH_2OH)_2$	$(CH_2OH)_2$	[23]
$(CH_2OH)_2$	CH_4, H_2CO, CH_3OH?, CO, CO_2, $C(O)CH_2OH$	$HC(O)CH_2OH$	[23]

References: [1] *Gomis et al.* (2004a,b); [2] *Moore and Hudson* (2000); [3] *Zheng et al*. (2006); [4] *Loeffler et al.* (2006a); [5] *Kaiser and Roessler* (1998); [6] *Mulas et al.* (1998); [7] *Moore and Hudson* (2003); [8] *Strazzulla et al.* (2002); [9] Hudson and Moore (unpublished work); [10] *Gerakines and Moore* (2001); [11] *Trottier and Brooks* (2004); [12] *Loeffler et al.* (2005); [13] *Brucato et al*. (1997); [14] *Moore et al.* (2003); [15] *Hudson and Moore* (2000); [16] *Palumbo et al.* (1999); [17] *Hudson and Moore* (2002); [18] *Strazzulla and Palumbo* (1998); [19] *Gerakines et al.* (2004); [20] *Hudson and Moore* (2004); [21] *Moore* (1984); [22] *Moore et al.* (2007); [23] *Hudson et al.* (2005).

H_2O-rich TNO ice then experiments show that C_2H_5OH (ethanol) will also be present. The relevant chemical reactions are similar to those already presented for the formation of ethanol from $H_2O + CH_4$ mixtures. Mid-IR studies of irradiated $H_2O + CH_3OH$ ices show that $C_2H_4(OH)_2$, ethylene glycol is produced (*Hudson and Moore,* 2000), presumably by radical-radical coupling

$$CH_3OH \rightarrow H + CH_2OH \text{ (twice)}$$
$$CH_2OH + CH_2OH \rightarrow C_2H_4(OH)_2$$

Unfortunately, neither near-IR spectra nor optical constants have been published for H_2O-rich ices containing either C_2H_5OH or $C_2H_4(OH)_2$, although some mid-IR spectra are available (*Hudson et al.,* 2005). This is an all-too-common situation for most known or suspected TNO ices.

Continuing down Table 3, extensive work has been published on both $H_2O + CO$ and $H_2O + CO_2$ ices. In the former, CO readily combines with H atoms to follow the sequence

$$CO \rightarrow HCO \rightarrow H_2CO \rightarrow CH_3O \text{ and/or } CH_2OH \rightarrow CH_3OH$$

leading to H_2CO (formaldehyde) and CH_3OH. Calculations of reaction yields are possible using intrinsic IR band strengths (*Hudson and Moore,* 1999). A similar sequence produces HCOOH (formic acid) by H and OH addition to CO (*Hudson and Moore,* 1999). In the case of $H_2O + CO_2$ ices, a major reaction product is H_2CO_3, carbonic acid, a molecule that long avoided direct laboratory detection. This molecule has been produced both photochemically and radiolytically, yields have been determined, its destruction rate has been measured, mid-IR band strengths are known, and isotopic variants have been examined. Enough is known about H_2CO_3 to safely predict that it will form in TNO ices containing H_2O and CO_2, and subjected to ionizing radiation (*Gerakines et al.,* 2000; *Brucato et al.,* 1997).

Mention already has been made of ammonia as a possible surface component of Quaoar (*Jewitt and Luu,* 2004), and there are reports of ammonia for Charon also (*Dumas et al.,* 2001; *Brown and Calvin,* 2000). In general, the radiation products of NH_3 ices have received little attention, although one would expect H_2 and N_2 to be formed and possibly N_2H_4 and NH_2OH as well. Radiolytic oxidation of NH_3 to form N_2 has been suggested (*Loeffler et al.,* 2006b) as a chemical energy source for the water ice plumes of Enceladus and to drive resurfacing on TNOs. Irradiation of $H_2O + NH_3$ mixtures demonstrates that ammonia is more easily lost than H_2O because of both a greater sputtering yield and a more effective chemical alteration. Thus the

TABLE 3. Radiation products from H_2O-dominated two-component ices.

Ice Mixture	Reaction Products Identified in Ices	References
$H_2O + CH_4$	CH_3OH, C_2H_5OH, C_2H_6, CO, CO_2	[1]
$H_2O + C_2H_6$	CH_4, C_2H_4, C_2H_5OH, CO, CO_2, CH_3OH	[2]
$H_2O + C_2H_2$	C_2H_5OH, CH_3OH, C_2H_6, C_2H_4, CO, CO_2, CH_4, C_3H_8, $HC(=O)CH_3$, $CH_2CH(OH)$	[1]
$H_2O + CO$	CO_2, HCO, H_2CO, CH_3OH, HCOOH, $HCOO^-$, H_2CO_3	[3]
$H_2O + CO_2$	H_2CO_3, CO, O_3, H_2O_2	[4,5]
$H_2O + H_2CO$	CO, CO_2, CH_3OH, HCO, HCOOH, CH_4	[3]
$H_2O + CH_3OH$	CO, CO_2, H_2CO, HCO, CH_4, $C_2H_4(OH)_2$, $HCOO^-$	[6,7]
$H_2O + O_2$	O_3, H_2O_2, HO_2, HO_3	[8,9]
$H_2O + N_2$	H_2O_2	[8]
$H_2O + NH_3$	NH_4^+	[2,10]
$H_2O + HCN$	CN^-, HNCO, OCN^-, $HC(=O)NH_2$, NH_4^+ (?), CO, CO_2	[11]
$H_2O + CH_3CN$	H_2CCNH, CH_4, OCN^-, HCN	[12]
$H_2O + HCCCN$	OCN^-	[12]
$H_2O + HNCO$	NH_4^+, OCN^-, CO, CO_2	[2]
$H_2O + SO_2$	H_3O^+, SO_4^{2-}, HSO_4^{2-}, HSO_3^{2-}	[13]
$H_2O + H_2S$	H_2S_2, SO_2	[13]
$H_2O + OCS$	CO, CO_2, SO_2, H_2CO (?), H_2O_2 (?)	[2]
$H_2O + HC(O)CH_2OH$	CO, CO_2	[14]
$H_2O + (CH_2OH)_2$	CO, CO_2, H_2CO, $HC(O)CH_2OH$	[14]

References: [1] *Moore and Hudson* (1998); [2] Hudson and Moore (unpublished data); [3] *Hudson and Moore* (1999); [4] *Brucato et al*. (1997); [5] *Gerakines et al*. (2000); [6] *Hudson and Moore* (2000); [7] *Palumbo et al*. (1999); [8] *Moore and Hudson* (2000); [9] *Cooper et al.* (2006b); [10] *Strazzulla and Palumbo* (1998); [11] *Gerakines et al.* (2004); [12] *Hudson and Moore* (2004); [13] *Moore et al.* (2007); [14] *Hudson et al.* (2005).

water/ammonia ratio progressively increases with radiation dose, and ammonia IR bands become less evident in transmission mid-IR spectra (*Strazzulla and Palumbo,* 1998). The observation of ammonia or an ammonia hydrate on TNO surfaces (e.g., on Quaoar) would then be evidence for a fresh exposed surface.

Ammonia also should play a role in the acid-base chemistry of TNO ices and experiments support this expectation. Irradiation of H_2O + CO ices produces HCOOH (formic acid), but similar experiments on H_2O + CO + NH_3 mixtures show no HCOOH but rather the $HCOO^-$ (formate) and NH_4^+ (ammonium) ions, as seen in Fig. 4 (*Hudson and Moore,* 2000). These ions are sufficiently stable, so as to accumulate on a TNO surface, or anywhere that sufficient energetic processing occurs. Beyond NH_4^+, other ions that have been studied in laboratory H_2O-rich ices include OCN^- from HNCO (*Hudson et al.,* 2001) and CN^- from HCN (*Moore and Hudson,* 2003). An earlier survey reported a near-IR band for NH_4^+, but nothing distinct for the other ions already mentioned (*Moore et al.,* 2003). Older laboratory work (*Maki and Decius,* 1958) shows that OCN^- may have near-IR bands suitable for searches in TNO spectra, but the experiments need to be repeated at more relevant temperatures and in the presence of H_2O-ice. H_3O^+ and OH^- also are likely in TNO ices, but difficult to detect by IR methods as they lack strong unobscured bands.

Of the organics remaining in Table 3 we mention only the nitriles, molecules containing the C≡N functional group. Ion-irradiated and UV-photolyzed nitrile-containing ices recently have been studied to understand their fate in H_2O-rich environments (*Hudson and Moore,* 2004). In all cases, nitriles were found to be unstable toward oxidation to OCN^-. This observation makes it unlikely that nitriles will be found in H_2O-rich TNO ices. Energetic processing also was found to give the H-atom transfer $CH_3CN \rightarrow H_2C{=}C{=}NH$ (keteni-

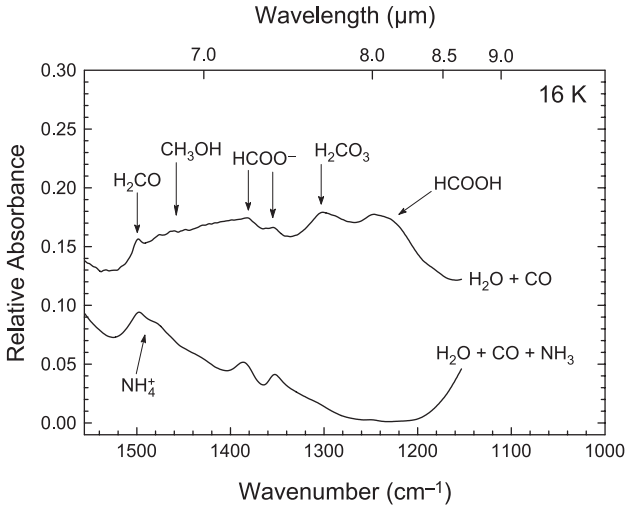

Fig. 4. IR spectra of two irradiated laboratory ices at 16 K, showing the influence of acid-base chemistry. The upper trace is an H_2O + CO (5:1) ice and the lower trace is an H_2O + CO + NH_3 (5:1:1) ice. Both were irradiated to about 22 eV 16-amu molecule^{-1} (after *Hudson et al.,* 2001).

mine). While CH_3CN (acetonitrile) has long been known in interstellar clouds, H_2CCNH has not, and so was predicted on the basis of the experiments (*Hudson and Moore,* 2004). Its recent discovery toward the star-forming region Sagittarius B2(N) (*Lovas et al.,* 2006) attests to the predictive power of the experimental approach.

Finally, Table 3 includes results from three sulfur-containing molecules, H_2S, OCS, and SO_2. All are known to be present both in comets and the interstellar medium, and OCS has been reported in the solid phase (*Palumbo et al.,* 1997). Given the oxidative power of ion-irradiated H_2O-ice, it is not surprising that the $H_2S \rightarrow SO_2 \rightarrow SO_4^{2-}$ sequence was found in recent laboratory measurements (*Moore et al.,* 2007). The implication for TNOs is that sulfur may well be present as SO_4^{2-}, similar to what is seen for Europa (*Carlson et al.,* 1999b).

4.4. Chemistry of N_2-rich Ice Mixtures

As already mentioned, models of Pluto and Triton spectra suggest that some TNO surfaces are dominated by N_2. Unfortunately, laboratory studies of N_2-rich ices are far fewer in number than those for H_2O-rich ices. Only a few examples of N_2-rich ice chemistry will be given here, involving CH_4 and CO (*Moore and Hudson,* 2003; *Palumbo et al.,* 2004).

Ion-irradiated $N_2 + CH_4$ ices near 12 K produce nitrogen-containing products HCN, HNC, and CH_2N_2, as well as NH_3 (*Moore and Hudson,* 2003). In addition, several hydrocarbons are identified, but their abundances depend on the initial N_2/CH_4 ratio. Figure 5 shows the 2.8–4-μm region of an irradiated $N_2 + CH_4$ mixture for three different initial N_2/CH_4 ratios, 100, 50, and 4, compared to pure irradiated CH_4. The abundances of aliphatic hydrocarbons, C_2H_6 and C_3H_8, are enhanced as the concentration of CH_4 increases. Therefore, TNO terrains rich in CH_4 are expected to have more C_2H_6 and C_3H_8 than those where CH_4 is diluted in N_2. When these ices are warmed to ~35 K, sharp features of HCN and HNC decrease as acid-based reactions produce both NH_4^+ and CN^- ions. Since these ions are stable under vacuum to about 150 K, they can accumulate on TNO surfaces. Diazomethane, CH_2N_2, also was seen in these experiments and was stable to at least ~35 K. The hydrocarbons C_2H_2, C_2H_6, and C_3H_8 are present to at least the 60–70 K range.

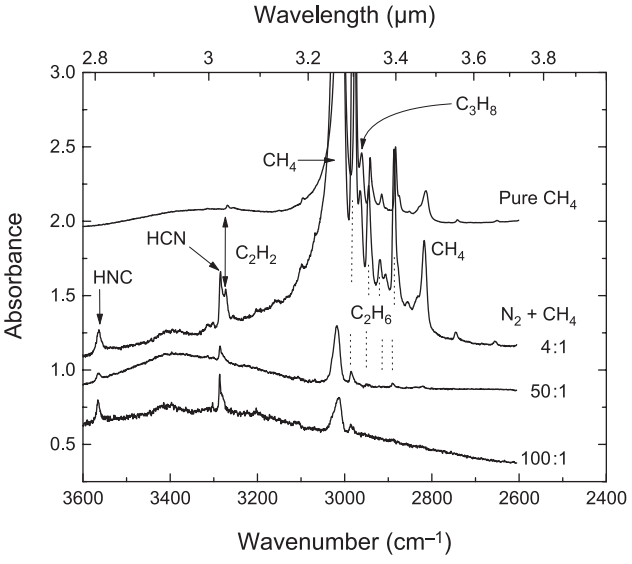

Fig. 5. Infrared spectra of 0.8 MeV irradiated pure CH_4 (top) and three $N_2 + CH_4$ mixtures. The formation of HCN, HNC, and hydrocarbons is indicated. The relative yields of HCN and HNC radiation products are greatest for the 100:1 mixture (*Moore and Hudson,* 2003).

Ion irradiations of $N_2 + CO$ ices at 12 K produce the free radicals OCN, NO, NO_2, and N_3, as well as the C_3O_2 (carbon suboxide) and N_2O (nitrous oxide) molecules. The latter two are the species most likely to persist on TNO surfaces, the radicals being less stable (more reactive).

Mid-IR spectra of irradiated $N_2 + CO + CH_4$ ices are largely what would be expected from the binary mixtures just described. The main new product is HNCO, seen at 12 K. On warming to ~35 K, HNCO reacts with NH_3 to form OCN^- and NH_4^+, which are stable to about 200 K.

4.5. Residual Materials

It may be concluded from the foregoing that TNOs can possess surfaces made of both irradiated ices and residual species remaining after at least partial sublimation of more-volatile molecules such as N_2, CO, and CH_4. The sources of ions such as OCN^- CN^-, and NH_4^+ have already been discussed. Other molecules that might be residual materials include $C_2H_4(OH)_2$, C_3O_2, and H_2CO_3. Mid-IR band strengths have been published for all three, and near-IR values are available for the first two (*Moore et al.,* 2003; *Hudson et al.,* 2005).

In concluding this section we note that the doses used in most ice experiments are in the range of about 1–20 eV/16-amu-molecule. Doses of this size typically lead to a state of chemical equilibrium in which the ice's composition changes only very slowly. However, with increasing dose, and gradual loss of H_2, the carbon-to-hydrogen ratio of the original sample slowly rises (*Strazzulla et al.,* 1991). This process has important implications for understanding TNO surface colors and will be explored in the next section. Here we note that this carbonization is very different from the formation of specific long-chain molecules, such as polymeric HCN or polymeric H_2CO. Although the latter two polymers are sometimes invoked by astrochemists, the formation of unique polymeric materials in ice mixtures remains problematic.

5. SPECTROSCOPY AND TRANSNEPTUNIAN OBJECT COLORS

The measurements of irradiated ices just described were typically performed using transmission spectroscopy. We now turn to investigations of more-refractory materials, with

spectra often recorded as diffuse reflectance measurements in the visible and near-IR regions (0.3–2.7 μm). These experiments investigate TNO chemistry through the study of spectral features, and reveal radiation-induced color changes in the underlying spectral continuum of TNO candidate materials. Diffuse reflectance spectroscopy also allows opaque refractories, such as silicates and various carbonaceous materials, to be studied more easily than by transmission methods. That such materials are important for understanding TNO surfaces is shown by the fit of the observed spectrum of the Centaur object 5145 Pholus to olivine (a silicate), tholins (a refractory organic material), H_2O-ice, frozen methanol, and carbon black (see *Cruikshank et al.,* 1998).

Among the materials studied by reflectance are terrestrial silicates (e.g., olivine and pyroxene) and carbons (e.g., natural bitumens such as asphaltite and kerite), meteorites (carbonaceous chondrites, ordinary chondrites, diogenites), and frozen ices such as methanol, methane, and benzene. Samples have been irradiated with different ions (H^+, He^+, Ar^+, Ar^{++}) having energies from 30 to 400 keV. All these materials show important spectral changes in their underlying visible-near-IR continuum after irradiation, usually reddening and darkening. Natural bitumens (asphaltite and kerite), however, are a noteworthy exception, being very dark in the visible region and possessing red-sloped spectra in the visible and near-IR (*Moroz et al.,* 1998). Ion irradiation experiments (*Moroz et al.,* 2004) showed that radiation-induced carbonization can gradually neutralize these spectral slopes.

The spectral slopes of ion-irradiated silicatic materials, namely olivine, pyroxene, and the olivine-rich meteorite Epinal, have been compared with observations of some S-type near-Earth asteroids. It has been found that the formation of solid-phase vacancies by solar wind ions can redden surfaces on a timescale of about 10^5 yr (*Strazzulla et al.,* 2005b). This means that radiation processing is the most efficient explanation for the observed color variety of both near-Earth and S-type main-belt asteroids (*Strazzulla et al.,* 2005b; *Brunetto and Strazzulla,* 2005; *Marchi et al.,* 2005). As an example of this work, Fig. 6 shows reflectance spectra (0.7–2.7 μm; normalized to 1 at 0.7 μm) of the meteorite Epinal before and after ion irradiation. The spectral reddening is quite evident. Another example comes from ion bombardment experiments with two carbonaceous chondrites, CV3 Allende and CO3 Frontier Mountain 95002. This work showed that those meteorites also are reddened by irradiation, regardless of whether the sample was a powder or a pressed pellet (*Lazzarin et al.,* 2006).

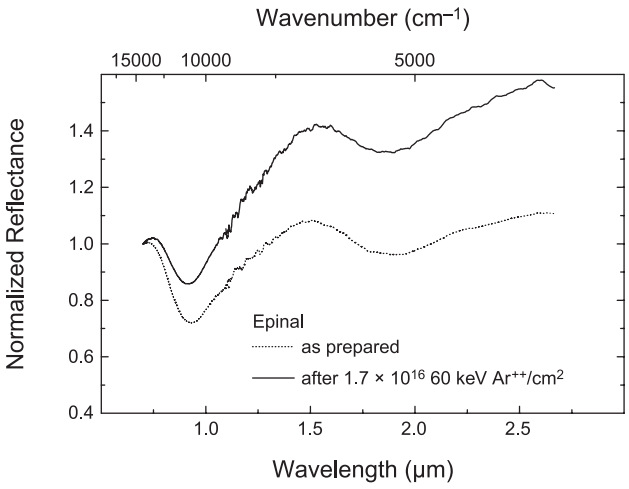

Fig. 6. Reflectance spectra (0.7–2.7 μm) of meteorite Epinal (H5) before and after ion irradiation. Spectra have been normalized to 1 at 0.7 μm (adapted from *Brunetto et al.,* 2005).

In addition to these results with complex starting materials, changes in colors also are found when fairly simple ices, such as CH_3OH, CH_4, C_6H_6, and $H_2O + CH_4 + N_2$ mixtures, are irradiated to doses of about 1000 eV/16-amu-molecule. Samples have been analyzed both by reflectance and Raman spectroscopies, and the formation of an organic refractory residue, and eventually the formation of amorphous carbon (*Ferini et al.,* 2004; *Palumbo et al.,* 2004), are seen. These materials cause a strong reddening and darkening of the visible and near-IR spectra (*Brunetto et al.,* 2006) of the original sample. Furthermore, *Brunetto et al.* (2006) showed that for these icy samples, it is the total dose (elastic plus inelastic contributions) that plays the main role in the reddening process. This is different from the case of silicates (*Brunetto and Strazzulla*, 2005) and bitumens (*Moroz et al.,* 2004), in which reddening effects are due solely to the elastic collisions between ions and target nuclei.

Figure 7 shows near-IR reflectance spectra of CH_4 and CH_3OH before and after irradiation at 16 K and 77 K, respectively. The spectra of the unprocessed ices are flat and bright, and show absorptions due to vibrational overtones and combinations. After irradiation, the original bands decrease and other features appear indicating the formation of new molecules discussed in section 4. Here we emphasize the change in the slope of the continuum after irradiation. It is clear from Fig. 7 that the spectrum of each compound becomes darker and redder with increasing dose.

Radiation-induced color variations have been compared with the observed spectra of some Centaurs and TNOs (after *Barucci and Peixinho,* 2005), and it has been shown (*Brunetto et al.,* 2006) that the observed TNO colors can be reproduced by ion irradiation experiments. This suggests that these objects possess a refractory organic crust developed after prolonged irradiation by cosmic ions, in analogy with what was previously suggested for Oort cloud comets (*Strazzulla et al.,* 1991). Many of the TNOs considered possess red colors that correspond to radiation doses between 10 and 100 eV/16-amu-molecule, but more-neutral-colored objects could have accumulated much higher dosages (*Moroz et al.,* 2003, 2004). It is estimated (*Strazzulla et al.,* 2003) that the surface layers (1–100 μm) of objects between 85 AU (solar wind termination shock) and the very local interstellar medium accumulate 100 eV/16-amu-molecule on timescales of 10^6–10^9 yr. This suggests that many icy objects in the outer solar system develop an irradiation mantle on

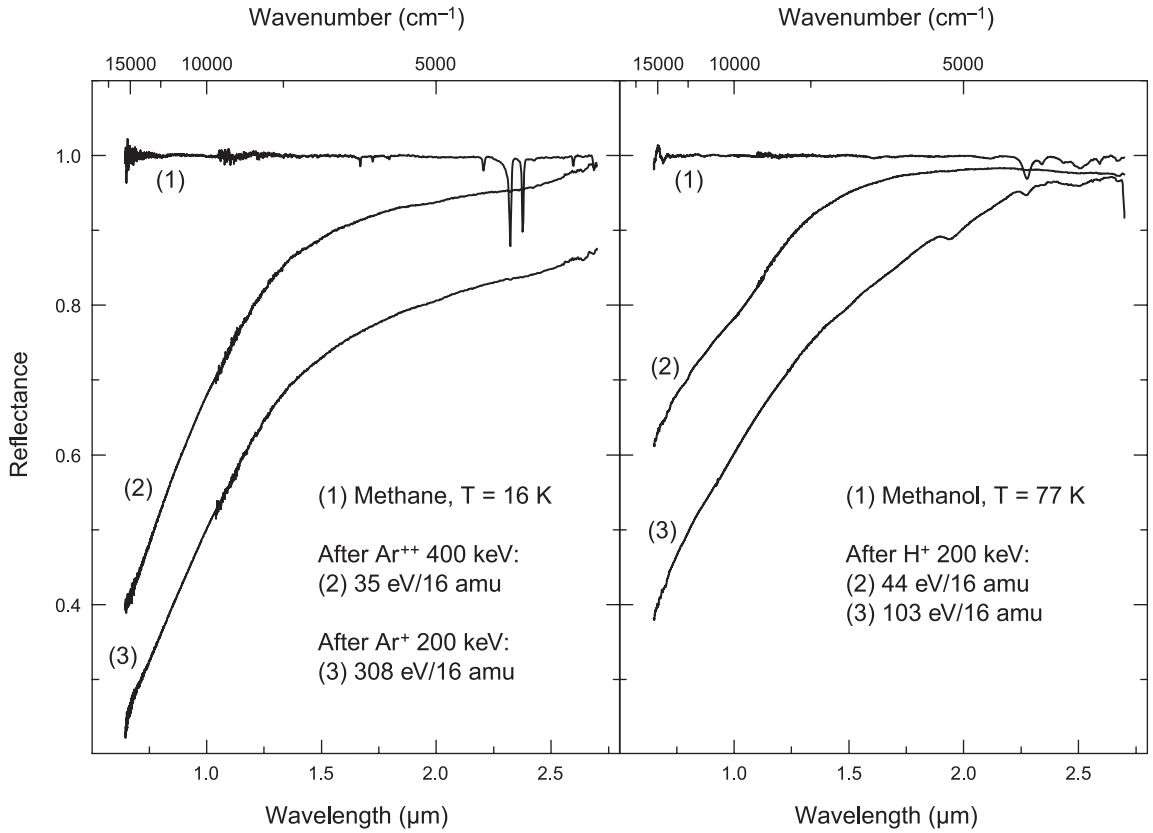

Fig. 7. Absolute visible-near-IR reflectance spectra of CH_4 (16 K) and CH_3OH (77 K) before and after irradiation with 200 keV Ar^+, 400 keV Ar^{++}, and 200 keV H^+ (adapted from *Brunetto et al.,* 2006).

timescales of 10^8 yr. From *Cooper et al*. (2003) and updates in Table 1, doses at 40–50 AU are lower, and volatile materials (e.g., N_2, CO, CH_4) can be better preserved at TNO surfaces.

The laboratory work summarized here and in section 4 implies that TNOs can possess a dark radiation mantle covering fresh subsurface ice hidden from observers. Transneptunian objects on which molecular ices (e.g., H_2O or CH_4) have been observed could either be poorly irradiated, have recently refreshed surfaces, and/or be lacking in carbon-bearing surface species to be converted into dark materials. In the first case, colored spectra are predicted depending on the surface portion recently refreshed. In the second case, spectra should be relatively flat with higher-than-average albedos.

Laboratory experiments also have shown that IR features of crystalline H_2O-ice are converted to those of amorphous material by irradiation at 10 K, that some crystalline IR features persist after irradiation at 50 K, and that at 70 K and higher the IR spectrum shows only slight changes (*Moore and Hudson,* 1992; *Strazzulla et al.,* 1992; *Mastrapa and Brown,* 2006). The observation of crystalline TNO H_2O-ice, in cases where it has been possible to distinguish between amorphous and crystalline material, is at present explained by freshly resurfaced layers (*Moore and Hudson,* 1992; *Strazzulla et al.,* 1992).

6. ASTROBIOLOGY

Important goals of astrobiology include understanding the origin of life on Earth and the possible forms of life present now, or in the past, on astronomical objects in and beyond the solar system. With this in mind, it must be admitted that TNO environments are very hostile to the origin or permanence of life as now exists on Earth. However, the possibility that terrestrial life, or the molecular ingredients from which such life originated, had an extraterrestrial source is actively debated. The "space vehicles" that could have delivered biologically relevant materials to the early Earth are thought to be meteorites, interplanetary dust particles, and comets from the Oort cloud and the Kuiper belt, supporting the relevance of TNOs to astrobiology.

A consideration of the chemistry reviewed in this chapter also supports the astrobiological importance of TNOs. First, the chemical processes in section 4, represented by products in Tables 2 and 3, are quite general for all irradiated ices. Reactions involving either bond breakage in a neutral molecule (e.g., $CH_3OH \rightarrow CO + 2\ H_2$) or the addition of a radical to a neutral (e.g., $H + CO \rightarrow HCO$) may require energy, but such can be provided by radiolysis. In contrast, little or no activation energy is encountered in most radical-radical combinations, proton transfers (acid-base reactions), or electron transfers (redox chemistry). Regard-

less of energetic considerations, all the aforementioned reactions are operative in irradiated ices, and do not depend on a reactant molecule's size. This implies that second- and third-generation products can form with accompanying increases in molecular complexity (e.g., chain length, molecular size, functional groups), albeit with lower yields. In this light, the reaction products seen to date are only the more-abundant ones in laboratory ices and, by extension, in TNO ices. This is important since biomolecules tend to be more complex than those found in either Table 2 or 3.

Many publications are available to support these points and to demonstrate biomolecular syntheses in ices, but only a few examples can be described here. Amino acids have been shown to form in processed ice mixtures after hydrolysis of the resulting radiation residues (*Kobayashi et al.,* 1995), while *Bernstein et al.* (2002) and *Muñoz Caro et al.* (2002) have found that UV-photolyzed ice mixtures contain precursors that lead to a suite of amino acids, some of which are found in meteorites. *Hudson et al.* (2005) reported the radiation synthesis of the simple sugar glycolaldehyde ($HOCH_2C(O)H$) in irradiated ethylene glycol, itself a product of CH_3OH radiolysis. Polycyclic aromatic hydrocarbon (PAH) molecules undergo sidegroup addition reactions to form alcohols, quinones, and ethers when irradiated in H_2O-ice (*Bernstein et al.,* 1999, 2003). *Tuleta et al.* (2001) studied the reaction products of simultaneously flowing H_2O vapor over 150-K anthracene (a PAH) and irradiating with 3.5-keV H_2^+ ions. Sidegroup addition to anthracene was found along with the oxidation product, anthraquinone.

In addition to experiments with icy mixtures, the growth of molecular chains, necessary for biomolecules to form, has been studied with model systems. *Strazzulla and Moroz* (2005) irradiated thin asphaltite films, both pure and covered with H_2O-ice layers. (Asphaltite was used as an analog of a complex carbonaceous material having both aliphatic and aromatic components.) After irradiation of both pure and H_2O-ice covered samples, carbon-carbon bonds characteristic of linear chains were found (carbynoids and cumulenes), as were new aromatic features. Low-temperature irradiations of solid acetylene (*Strazzulla et al.,* 2002), benzene, and cluster-assembled carbon thin films (*Strazzulla and Baratta,* 1991; *Strazzulla et al.,* 2005a) also showed evidence of carbon-chain extension, with the final products remaining present after warming the samples to ~300 K. The synthesis of such products appears to be typical of many irradiated hydrogen-bearing carbonaceous materials. The formation of carbon-carbon and carbon-nitrogen (section 4) triple bonds is particularly relevant to astrobiology. These materials, once delivered to the early Earth, could have been among the first ingredients to develop biochemical activity.

While the formation of larger structures from smaller ones is important, to understand equilibrium molecular abundances one must also understand destruction processes. As an example of how laboratory methods contribute to solving such problems, we end with the formamide molecule, $HCONH_2$. Formamide is made from the four major biogenic elements, has been observed in the interstellar medium (*Millar,* 2004), in the long-period comet C/1995 O1 Hale-Bopp (*Bockelée-Morvan et al.,* 2000), and tentatively in young stellar objects W33A (*Schutte et al.,* 1999) and NGC 7538 IRS9 (*Raunier et al.,* 2004). Formamide is made by room-temperature HCN hydrolysis, and it is the most-abundant pyrolysis product of HCN-polymer. Its role as a prebiotic precursor for the synthesis of nucleobases has been shown under a variety of conditions. In particular, various inorganic materials, such as cosmic-dust analogs, can catalyze formamide condensation to make many other compounds including purine and pyrimidine bases (*Brucato et al.,* 2006, and references therein). The radiation chemistry of frozen $HCONH_2$ has recently been studied at 20 K (*Brucato et al.,* 2006), and CO, CO_2, N_2O, isocyanic acid (HNCO), and ammonium cyanate ($NH_4^+OCN^-$) decomposition products were identified. Some of these species were stable even after warming to room temperature.

7. NEEDS AND CHALLENGES

Although extensive laboratory work has been done on solar system ice analogs, important and difficult tasks remain. High among these challenges is a clear demonstration of the extent and types of space weathering experienced by TNO surfaces. This chapter has documented some of the possible radiation-induced changes in spectra, colors, and chemical composition, but distinguishing these from other effects remains problematic.

Further quantification of previous work also needs to be done. Intrinsic strengths for many IR spectral features are known, but optical constants of many irradiated icy and refractory materials are needed. Only with laboratory optical constants of irradiated materials can such be included in quantitative models (e.g., Skuratov and Hapke) and fits of TNO spectra. However, the measurement of optical constants is difficult, and so many TNO candidate materials have not been studied.

The gaps in Table 2 and 3 also suggest avenues for future TNO ice experiments. Most entries in the tables come from publications covering only a few temperatures and but one radiation source. Additional work is needed to search for possible new product molecules, particularly those of astrobiological interest, and ions other than NH_4^+ and OCN^-.

We also note that there may be problems of scale to consider, since the behavior of deep-volume bulk ices irradiated at centimeter-to-meter depths by highly penetrating energetic particles and electromagnetic radiations is unknown. Input doses can be calculated with sophisticated radiation transport codes such as GEANT, but radiolytic yields can only be extrapolated from measurements on ices under ~1 mm in thickness. What are the long-range effects of penetrating particle ionization and mobile gas production in thicker ices? Are reaction rates enhanced by large internal surface areas in porous volume ice? Are chemical pathways altered by mobile electrons or H^+ in a bulk irradiated ice? Such questions require the transition of laboratory sample

and irradiation system dimensions from microscopic to macroscopic scales.

Finally, there is a need for the chemistry represented in sections 4 (ices) and 5 (refractories) to be united in future laboratory experiments. For example, how will reactions to extend the length of carbon chains be altered when H_2O-ice is present? Conversely, Table 3 documents the radiation products expected in various H_2O-rich ices, but to what extent will product distributions be different in the presence of refractory materials?

Acknowledgments. The work in the Laboratory of Experimental Astrophysics in Catania has been financially supported by the National Institute for Astrophysics (INAF) in the framework of a national project. R.L.H. and M.H.M. acknowledge support through NASA's Outer Planets, Planetary Atmospheres, and Planetary Geology and Geochemistry programs. Recent support through the NASA Astrobiology Institute's Goddard Center for Astrobiology is also acknowledged. J.F.C. acknowledges past or current support from NASA's Heliophysics, Jovian System Data Analysis, Planetary Atmospheres, and Outer Planets programs.

REFERENCES

Anders E. and Grevesse N. (1989) Abundances of the elements — meteoritic and solar. *Geochim. Cosmochim. Acta, 53,* 197–214.

Bagnulo S., Boehnhardt H., Muinonen K., Kolokolova L., Belskaya I., and Barucci M. A. (2006) Exploring the surface properties of transneptunian objects and Centaurs with polarimetric FORS1/VLT observations. *Astron. Astrophys., 450,* 1239–1248.

Baratta G. A. and Palumbo M. E. (1998) Infrared optical constants of CO and CO_2 thin icy films. *J. Opt. Soc. Am. A, 15,* 3076–3085.

Baratta G. A., Leto G., and Palumbo M. E. (2002) A comparison of ion irradiation and UV photolysis of CH_4 and CH_3OH. *Astron. Astrophys., 384,* 343–349.

Baratta G. A., Domingo M., Ferini G., Leto G., Palumbo M. E., Satorre M. A., and Strazzulla G. (2003) Ion irradiation of CH_4-containing icy mixtures. *Nucl. Instr. Meth. B, 209,* 283–287.

Barucci M. A. and Peixinho N. (2005) Trans-Neptunian objects' surface properties. In *Asteroids, Comets, Meteors* (D. Lazzaro et al., eds.), pp. 171–190. IAU Symposium No. 229, Cambridge Univ., Cambridge.

Bernstein M. P., Sandford S. A., Allamandola L. J., Gillette J. S., Clemett S. J., and Zare R. N. (1999) UV irradiation of polycyclic aromatic hydrocarbons in ices: Production of alcohols, quinones, and ethers. *Science, 283,* 1135–1138.

Bernstein M. B., Dworkin J. P., Sandford S. A., Cooper G. W., and Allamandola L. J. (2002) Racemic amino acids from the ultraviolet photolysis of interstellar ice analogues. *Nature, 416,* 401–403.

Bernstein M. P., Moore M. H., Elsila J. E., Sandford S. A., Allamandola L. J., and Zare R. N. (2003) Side group addition to the polycyclic aromatic hydrocarbon coronene by proton irradiation in cosmic ice analogs. *Astrophys. J. Lett., 582,* L25–L29.

Bernstein M. B., Cruikshank D. P., and Sandford S. A. (2005) Near-infrared laboratory spectra of solid H_2O/CO_2 and CH_3OH/CO_2 ice mixtures. *Icarus, 179,* 527–534.

Bernstein M. B., Cruikshank D. P., and Sandford S. A. (2006) Near-infrared spectra of laboratory H_2O-CH_4 ice mixtures. *Icarus, 181,* 302–208.

Bockelée-Morvan D., Lis D. C., Wink J. E., Despois D., Crovisier J., Bachiller R., Benford D. J., Biver N., Colo P., Davies J. K., Gérard E., Germain B., Houde M., Mehringer D., Moreno R., Paubert G., Phillip T. G., and Raue H. (2000) New molecules found in comet C/1995 O1 (Hale-Bopp). Investigating the link between cometary and interstellar material. *Astron. Astrophys., 353,* 1101–1114.

Brown M. E. and Calvin W. M. (2000) Evidence for crystalline water and ammonia ices on Pluto's satellite Charon. *Science, 287,* 107–109.

Brown R. H., Cruikshank D. P., and Pendleton Y. (1999) Water ice on Kuiper belt object 1996 TO_{66}. *Astrophys. J. Lett., 519,* L101–L104.

Brucato J. R., Palumbo M. E., and Strazzulla G. (1997) Carbonic acid by ion implantation in water/carbon dioxide ice mixtures. *Icarus, 125,* 135–144.

Brucato J. R., Baratta G. A., and Strazzulla G. (2006) An infrared study of pure and ion irradiated frozen formamide. *Astron. Astrophys., 455,* 395–399.

Brunetto R. and Strazzulla G. (2005) Elastic collisions in ion irradiation experiments: A mechanism for space weathering of silicates. *Icarus, 179,* 265–273.

Brunetto R., Orofino V., and Strazzulla G. (2005) Space weathering on minor bodies induced by ion irradiation: Some experimental results. *Mem. S. A. Ital. Suppl., 6,* 45–50.

Brunetto R., Barucci M. A., Dotto E., and Strazzulla G. (2006) Ion irradiation of frozen methanol, methane, and benzene: Linking to the colors of Centaurs and trans-Neptunian objects. *Astrophys. J., 644,* 646–650.

Burlaga L. F., Ness N. F., Acuna M. H., Lepping R. P., Connerney J. E. P., Stone E. C., and McDonald F. B. (2005) Crossing the termination shock into the heliosheath: Magnetic fields. *Science, 309,* 2027–2029.

Carlson R. W., Anderson M. S., Johnson R. E., Smythe W. D., Hendrix A. R., Barth C. A., Soderblom L. A., Hansen G. B., McCord T. B., Dalton J. B., Clark R. N., Shirley J. H., Ocampo A. C., and Matson D. L. (1999a) Hydrogen peroxide on Europa. *Science, 283,* 2062–2064.

Carlson R. W., Johnson R. E., and Anderson M. S. (1999b) Sulfuric acid on Europa and the radiolytic sulfur cycle. *Science, 286,* 97–99.

Colangeli L., Brucato J. R., Bar-Nun A., Hudson R. L., and Moore M. H. (2005) Laboratory experiments on cometary materials. In *Comets II* (M. C. Festou et al., eds.), pp. 695–717. Univ. of Arizona, Tucson.

Cooper J. F., Johnson R. E., Mauk B. H., Garrett H. B., and Gehrels N. (2001) Energetic ion and electron irradiation of the icy Galilean satellites. *Icarus, 149,* 133–159.

Cooper J. F., Christian E. R., Richardson J. D., and Wang C. (2003) Proton irradiation of Centaur, Kuiper belt, and Oort cloud objects at plasma to cosmic ray energy. *Earth Moon Planets, 92,* 261–277.

Cooper J. F., Hill M. E., Richardson J. D., and Sturner S. J. (2006a) Proton irradiation environment of solar system objects in the heliospheric boundary regions. In *Physics of the Inner Heliosheath* (J. Heerikhuisen et al., eds.), pp. 372–379. AIP Conf. Proc. 858, American Institute of Physics, New York.

Cooper P. D., Moore M. H., and Hudson R. L. (2006b) Infrared detection of HO_2 and HO_3 radicals in water ice. *J. Phys. Chem. A, 110,* 7985–7988.

Cruikshank D. P., Roush T. L., Owen T. C., Geballe T. R., de Bergh C., Schmitt B., Brown R. H., and Bartholomew M. J. (1993) Ices on the surface of Triton. *Science, 261,* 742–745.

Cruikshank D. P., Roush T. L., Bartholomew M. J., Geballe T. R., Pendleton Y. J., White S. M., Bell J. F. III, Davies J. K., Owen T. C., de Bergh C., Tholen D. J., Bernstein M. P., Brown R. H., Tryka K. A., and Dalle Ore C. M. (1998) The composition of Centaur 5145 Pholus. *Icarus, 135,* 389–407.

Decker R. B., Krimigis S. M., Roelof E. C., Hill M. E., Armstrong T. P., Gloeckler G., Hamilton D. C., and Lanzerotti L. J. (2005) Voyager 1 in the foreshock, termination shock, and heliosheath. *Science, 309,* 2020–2024.

Douté S., Schmitt B., Quirico E., Owen T. C., Cruikshank D. P., de Bergh C., Geballe T. R., and Roush T. L. (1999) Evidence for methane segregation at the surface of Pluto. *Icarus, 142,* 421–444.

Dumas C., Terrile R. J., Brown R. H., Schneider G., and Smith B. A. (2001) Hubble Space Telescope NICMOS spectroscopy of Charon's leading and trailing hemispheres. *Astrophys. J., 121,* 1163–1170.

Elliot J. L. and Kern S. D. (2003) Pluto's atmosphere and a targeted-occultation search for other bound KBO atmospheres. *Earth Moon Planets, 92,* 375–393.

Ferini G., Baratta G. A., and Palumbo M. E. (2004) A Raman study of ion irradiated icy mixtures. *Astron. Astrophys., 414,* 757–766.

Gerakines P. A. and Moore M. H. (2001) Carbon suboxide in astrophysical ice analogs. *Icarus, 154,* 372–380.

Gerakines P. A., Moore M. H., and Hudson R. L. (2000) Carbonic acid production in $H_2O + CO_2$ ices: UV photolysis vs. proton bombardment. *Astron. Astrophys., 357,* 793–800.

Gerakines P. A., Moore M. H., and Hudson R. L. (2004) Ultraviolet photolysis and proton irradiation of astrophysical ice analogs containing hydrogen cyanide. *Icarus, 170,* 204–213.

Gerakines P. A., Bray J. J., Davis A., and Richey C. R. (2005) The strengths of near-infrared absorption features relevant to interstellar and planetary ices. *Astrophys. J., 620,* 1140–1150.

Gomis O., Satorre M. A., Strazzulla G., and Leto G. (2004a) Hydrogen peroxide formation by ion implantation in water ice and its relevance to the Galilean satellites. *Planet. Space Sci., 52,* 371–378.

Gomis O., Leto G., and Strazzulla G. (2004b) Hydrogen peroxide production by ion irradiation of thin water ice films. *Astron. Astrophys., 420,* 405–410.

Grundy W. M., Buie M. W., and Spencer J. R. (2002) Spectroscopy of Pluto and Triton at 3–4 microns: Possible evidence for wide distribution of nonvolatile solids. *Astron. J., 124,* 2273–2278.

Hall L. A., Heroux L. J., and Hinterregger H. E. (1985) Solar ultraviolet irradiance. In *Handbook of Geophysics and the Space Environment* (A. S. Jura, ed.), pp. 2-1 to 2-21. Air Force Geophysics Laboratory, Hanscom AFB, Massachusetts.

Hudson R. L. and Moore M. H. (1999) Laboratory studies of the formation of methanol and other organic molecules by water + carbon monoxide radiolysis: Relevance to comets, icy satellites, and interstellar ices. *Icarus, 140,* 451–461.

Hudson R. L. and Moore M. H. (2000) IR spectra of irradiated cometary ice analogues containing methanol: A new assignment, a reassignment, and a nonassignment. *Icarus, 145,* 661–663.

Hudson R. L. and Moore M. H. (2002) The N_3 radical as a discriminator between ion-irradiated and UV-photolyzed astronomical ices. *Astrophys. J., 568,* 1095–1099.

Hudson R. L. and Moore M. H. (2004) Reactions of nitriles in ices relevant to Titan, comets, and the interstellar medium: Formation of cyanate ion, ketenimines, and isonitriles. *Icarus, 172,* 466–478.

Hudson R. L. and Moore M. H. (2006) Infrared spectra and radiation stability of H_2O_2 ices relevant to Europa. *Astrobiology, 6,* 48–489.

Hudson R. L., Moore M. H., and Gerakines P. A. (2001) The formation of cyanate ion (OCN^-) in interstellar ice analogues. *Astrophys. J., 550,* 1140–1150.

Hudson R. L., Moore M. H., and Cook A. M. (2005) IR characterization and radiation chemistry of glycolaldehyde and ethylene glycol ices. *Adv. Space Res., 36,* 184–189.

Jewitt D. C. and Luu J. (2004) Crystalline water ice on the Kuiper belt object (50000) Quaoar. *Nature, 432,* 731–733.

Johnson R. E. (1990) *Energetic Charged Particle Interactions with Atmospheres and Surfaces.* Springer-Verlag, Heidelberg.

Johnson R. E. (1995) Sputtering of ices in the outer solar system. *Rev. Mod. Phys., 68,* 305–312.

Johnson R. E., Cooper P. D., Quickenden T. I., Grieves G. A., and Orlando T. M. (2005) Production of oxygen by electronically induced dissociations in ice. *J. Chem. Phys., 123,* 184715-1 to 184715-8.

Kaiser R. I. and Roessler K. (1998) Theoretical and laboratory studies on the interaction of cosmic-ray particles with interstellar ices. III. Suprathermal chemistry-induced formation of hydrocarbon molecules in solid methane, (CH_4), ethylene (C_2H_4), and acetylene (C_2H_2). *Astrophys. J., 503,* 959–975.

Kerkhof O., Schutte W. A., and Ehrenfreund P. (1999) The infrared band strengths of CH_3OH, NH_3, and CH_4 in laboratory simulations of astrophysical ice mixtures. *Astron. Astrophys., 346,* 990–994.

Kobayashi K., Kasamatsu T., Kaneko T., Koike J., Oshima T., Sait T., Yamamoto T., and Yanagawa H. (1995) Formation of amino acid precursors in cometary ice environments by cosmic radiation. *Adv. Space Res.,162,* 21–26.

Lazzarin M., Marchi S., Moroz L., Brunetto R., Magrin S., Paolicchi P., and Strazzulla G. (2006) Space weathering in the main asteroid belt: The big picture. *Astrophys. J. Lett., 647,* L179–L182.

Licandro J., Pinella-Alonso N., Pedani M., Oliva E., Tozzi G. P., and Grundy W. M. (2006) The methane ice rich surface of large TNO 2005 FY_9: A Pluto-twin in the trans-Neptunian belt? *Astron. Astrophys., 445,* L35–L38.

Loeffler M. J., Baratta G. A., Palumbo M. E., Strazzulla G., and Baragiola R. A. (2005) CO_2 synthesis in solid CO by Lyman-alpha photons and 200 keV protons. *Astron. Astrophys., 435,* 587–594.

Loeffler M. J., Raut U., Vidal R. A., Baragiola R. A., and Carlson R. W. (2006a) Synthesis of hydrogen peroxide in water ice by ion irradiation. *Icarus, 180,* 265–273.

Loeffler M. J., Raut U., and Baragiola R. A. (2006b) Enceladus: A source of nitrogen and an explanation for the water. *Astrophys. J. Lett., 649,* L133–L136.

Lovas F. J., Hollis J. M., Remijan A. J., and Jewell P. R. (2006) Detection of keteneimine (CH_2CNH) in SgrB2(N) hot cores. *Astrophys. J. Lett., 645,* L137–L140.

Maki A. and Decius J. C. (1958) Infrared spectrum of cyanate ion as a solid solution in a potassium iodide lattice. *J. Chem. Phys., 28,* 1003–1004.

Marchi S., Brunetto R., Magrin S., Lazzarin M., and Gandolfi D.

(2005) Space weathering of near-Earth and main belt silicate-rich asteroids: Observations and ion irradiation experiments. *Astron. Astrophys., 443,* 769–775.

Mastrapa R. M. E. and Brown R. H. (2006) Ion irradiation of crystalline H_2O ice: Effect on the 1.65-μm band. *Icarus, 183,* 207–214.

Millar T. J. (2004) Organic molecules in the interstellar medium. In *Astrobiology: Future Perspectives* (P. Ehrenfreund et al., eds.), p. 17. Astrophysics and Space Science Library, Vol. 305, Kluwer, Dordrecht.

Moore M. H. (1984) Infrared studies of proton irradiated SO_2 ices: Implications for Io. *Icarus, 59,* 114–128.

Moore M. H. and Hudson R. L. (1992) Far-infrared spectral studies of phase changes in water ice induced by proton irradiation. *Astrophys. J., 401,* 353–360.

Moore M. H. and Hudson R. L. (1998) Infrared study of ion irradiated water ice mixtures with organics relevant to comets. *Ica-rus, 135,* 518–527.

Moore M. H. and Hudson R. L. (2000) IR detection of H_2O_2 at 80 K in ion-irradiated ices relevant to Europa. *Icarus, 145,* 282–288.

Moore M. H. and Hudson R. L. (2003) Infrared study of ion-irradiated N_2-dominated ices relevant to Triton and Pluto: Formation of HCN and HNC. *Icarus, 161,* 486–500.

Moore M. H., Hudson R. L., and Ferrante R. F. (2003) Radiation products in processed ices relevant to Edgeworth-Kuiper-belt objects. *Earth Moon Planets, 92,* 291–306.

Moore M. H., Hudson R. L., and Carlson R. W. (2007) The radiolysis of SO_2 and H_2S in water ice: Implications for the icy jovian satellites. *Icarus, 189,* 409–423.

Moroz L. V., Arnold G., Korochantsev A. V., and Wasch R. (1998) Natural solid bitumens as possible analogs for cometary and asteroid organics. *Icarus, 134,* 253–268.

Moroz L. V., Baratta G., Distefano E., Strazzulla G., Dotto E., and Barucci M. A. (2003) Ion irradiation of asphalite: Optical effects and implications for trans-neptunian objects and Centaurs. *Earth Moon Planets, 92,* 279–289.

Moroz L., Baratta G. A., Strazzulla G., Starukhina L., Dotto E., Barucci M. A., Arnold G., and Distefano E. (2004) Optical alteration of complex organics induced by ion irradiation: 1. Laboratory experiments suggest unusual space weathering trend. *Icarus, 170,* 214–228.

Mulas G., Baratta G. A., Palumbo M. E., and Strazzulla G. A. (1998) Profile of CH_4 IR bands in ice mixtures. *Astron. Astrophys., 333,* 1025–1033.

Mumma M. J., DiSanti M. A., Dello Russo N., Fomenkova M., Magee-Sauer K., Kaminski C. D., and Xie D. X. (1996) Detection of abundant ethane and methane, along with carbon monoxide and water, in Comet C/1996 B2 Hyakutake: Evidence for interstellar origin. *Science, 272,* 1310–1314.

Muñoz Caro G. M., Meierhenrich U. J., Schutte W. A., Barbier B., Arcones Segovia A., Rosenbauer H., Thiemann W. H.-P, Brack A., and Greenberg J. M. (2002) Amino acids from ultraviolet irradiation of interstellar ice analogues. *Nature, 416,* 403–406.

Owen T. C., Roush T. L., Cruikshank D. P., Elliot J. L., Young L. A., de Bergh C., Schmitt B., Geballe T. R., Brown R. H., and Bartholomew M. J. (1993) Surface ices and the atmospheric composition of Pluto. *Science, 261,* 745–748.

Palumbo M. E., Geballe T. R., and Tielens A. G. G. M. (1997) Solid carbonyl sulfide (OCS) in dense molecular clouds. *Astrophys. J., 479,* 839–844.

Palumbo M. E., Castorina A. C., and Strazzulla G. (1999) Ion irradiation effects on frozen methanol (CH_3OH). *Astron. Astrophys., 342,* 551–562.

Palumbo M. E., Ferini G., and Baratta G. A. (2004) Infrared and Raman spectroscopies of refractory residues left over after ion irradiation of nitrogen-bearing icy mixtures. *Adv. Space Res., 33,* 49–56.

Porco C. C., et al. (2006) Cassini observes the active south pole of Enceladus. *Science, 311,* 1393–1401.

Quirico E., Douté S., Schmitt B., de Bergh C., Cruikshank D. P., Owen T. C., Geballe T., and Roush T. L. (1999) Composition, physical state, and distribution of ices at the surface of Triton. *Icarus, 139,* 159–178.

Raunier S., Chiavassa T., Duvernay F., Borget F., Aycard J. P., Dartois E., and d'Hendecourt L. (2004) Tentative identification of urea and formamide in ISO-SWS infrared spectra of interstellar ices. *Astron. Astrophys., 416,* 165–169.

Sasaki T., Kanno A., Ishiguro M., Kinoshita D., and Nakamura R. (2005) Search for nonmethane hydrocarbons on Pluto. *Astrophys. J. Lett., 618,* L57–L60.

Schutte W. A., Boogert A. C. A., Tielens A. G. G. M., Whittet D. C. B., Gerakines P. A., Chiar J. E., Ehrenfreund P., Greenberg J. M., van Dishoeck E. F., and de Graauw, Th. (1999) Weak ice absorption features at 7.24 and 7.41 μm in the spectrum of the obscured young stellar object W 33A. *Astron. Astrophys., 343,* 966–976.

Stone E. C., Cummings A. C., McDonald F. B., Heikkila B. C., Lal N., and Webber W. R. (2005) Voyager 1 explores the termination shock region and the heliosheath beyond. *Science, 309,* 2017–2020.

Strazzulla G. and Baratta G. A. (1991) Laboratory study of the IR spectrum of ion-irradiated frozen benzene. *Astron. Astrophys., 241,* 310–316.

Strazzulla G. and Moroz L. (2005) Ion irradiation of asphaltite as an analogue of solid hydrocarbons in the interstellar medium. *Astron. Astrophys., 434,* 593–598.

Strazzulla G. and Palumbo M. E. (1998) Evolution of icy surfaces: An experimental approach. *Planet. Space Sci., 46,* 1339–1348.

Strazzulla G., Baratta G. A., Johnson R. E., and Donn B. (1991) Primordial comet mantle — Irradiation production of a stable, organic crust. *Icarus, 91,* 101–104.

Strazzulla G., Baratta G. A., Leto G., and Foti G. (1992) Ion-beam-induced amorphization of crystalline water ice. *Europhys. Lett., 18,* 517–522.

Strazzulla G., Baratta G. A, Domingo M., and Satorre M. A. (2002) Ion irradiation of frozen C_2H_n (n = 2, 4, 6). *Nucl. Instr. Meth. B, 191,* 714–717.

Strazzulla G., Cooper J. F., Christian E. R., and Johnson R. E. (2003) Ion irradiation of TNOs: From the fluxes measured in space to the laboratory experiments. *Compt. Rend. Phys., 4,* 791–801.

Strazzulla G., Baratta G. A., Battiato S., and Compagnini G. (2005a) Ion irradiations of solid carbons. In *Polyynes: Synthesis, Properties, and Applications* (F. Cataldo, ed.), pp. 271–284. CRC, New York.

Strazzulla G., Dotto E., Binzel R., Brunetto R., Barucci M. A., Blanco A., and Orofino V. (2005b) Spectral alteration of the meteorite Epinal (H5) induced by heavy ion irradiation: A simulation of space weathering effects on near-Earth asteroids. *Icarus, 174,* 31–35.

Sturner S. J., Shrader C. R., Weidenspointner G., Teegarden B. J., Attié D., et al. (2003) Monte Carlo simulations and genera-

tion of the SPI response. *Astron. Astrophys., 411,* L81–L84.

Tobiska W. K. and Bouwer S. D. (2006) New developments in SOLAR2000 for space research and operations. *Adv. Space Res., 37,* 347–358.

Tobiska W. K., Woods T., Eparvier F., Viereck R., Floyd L., Bouwer D., Rottman G., and White O. R. (2000) The SOLAR2000 empirical solar irradiance model and forecast tool. *J. Atmos. Solar Terr. Phys., 62,* 1233–1250.

Trottier A. and Brooks R. L. (2004) Carbon-chain oxides in proton-irradiated CO ice films. *Astrophys. J., 612,* 1214–1221.

Trujillo C. A., Brown M. E., Barkume K. M., Schaller E. L., and Rabinowitz D. L. (2007) The surface of 2003 EL_{61} in the near infrared. *Astrophys. J., 655,* 1172–1178.

Tuleta M., Gabla L., and Madej J. (2001) Bioastrophysical aspects of low energy ion irradiation of frozen anthracene containing water. *Phys. Rev. Lett., 87,* id. 078103.

Wada A., Mochizuki N., and Hiraoka K. (2006) Methanol formation from electron-irradiated mixed H_2O/CH_4 ice at 10 K. *As-trophys. J., 644,* 300–306.

Waite J. H., et al. (2006) Cassini Ion and Neutral Mass Spectrometer: Enceladus plume composition and structure. *Science, 311,* 1419–1422.

Weaver H. A., Brooke T. Y., Chin G., Kim S. J., Bockelée-Morvan D., and Davies J. K. (1998) Infrared spectroscopy of Comet Hale-Bopp. *Earth Moon Planets, 78,* 71–80.

Zheng W., Jewitt D., and Kaiser R. I. (2006) Temperature dependence of the formation of hydrogen, oxygen, and hydrogen peroxide in electron-irradiated crystalline water ice. *Astrophys. J., 648,* 753–761.

Ziegler J. F., Biersack J. P., and Littmark U. (1985) *The Stopping and Range of Ions in Solids.* Pergamon, New York.